3
Experimental procedures

This chapter describes the experimental setup and procedures used in the study of turbulent drop breakup of single droplets and diluted O/W emulsions for the two cases considered in this dissertation (breakup in a RSM and breakup through an orifice in a pipe). First, the properties of the materials and the techniques used for their determination are discussed. In the second subsection, the fundamental theory of pendant drop technique and interfacial tension measurements are reviewed. Then, the emulsions characterization methods and the experimental protocols that were applied in order to perform the visualization of breakup mechanisms for both cases evaluated in this study are specified. The final section explains the experimental procedures used to determine the Maximum Stable Drop Diameter (MSDD) in the turbulent breakup of diluted emulsions in the two cases considered in this work.

3.1
Materials

In this section, the nature and properties of the liquid phases that form the emulsions are described.

3.1.1
Continuous phases

Two types of continuous phases were used in the experimental work of this investigation. The first one, a surfactant based continuous phase, was a solution of the anionic commercial surfactant STEOL CS-330 (Sodium Lauryl Ether Sulfate derived from fatty alcohols, ethoxylated to an average of 3 moles and manufactured by Stepan® Company) in substitute ocean water. The surfactant concentration in the solution was 1122.5 mg/L (2.5 times the Critical Micelle Concentration). The substitute ocean water was prepared following the indications given by the ASME D1141-98 Standard (with exception of stock solution number

3) and its density and viscosity were estimated using the theory given by Sverdrup, Johnson and Fleming (1942) for a salinity of 35 g/Kg (estimated from chemical composition).

The second type of continuous phase was tap water, used in the visualization experiments for the case of high interfacial tension systems. Its density and viscosity were obtained from CRC Handbook of Chemistry and Physics (http://www.hbcpnetbase.com/). Finally, the electrical conductivity and pH values of both continuous phases were measured in the Oakton PC700 pH/mV/Conductivity/°F/°C bench meter. The properties of STEOL CS-330 and continuous phases are given in Tables 3.1 and 3.2, respectively.

Table 3. 1 STEOL CS-330 properties. T = 25 °C.
Source:http://www.stepan.com/pdfs/Bulletins/STEOLCS330.pdf

Property	Value
Appearance	Clear liquid
Actives (MW 422), %	28
pH, 10% Aqueous	7.5
Density, Kg/m^3	1030
Viscosity, Pa.s	0.062
Critical Micelle Concentration, mg/L	449

Table 3. 2 Physicochemical properties of continuous phases. T = 25 °C.

Property	Continuous phase	
	Surfactant based	Tap water
Density, Kg/m^3	1035	998
Dynamic Viscosity, Pa.s	0.00108	0.001
Electrical Conductivity, µS	53.2	0.144
pH	8.2	6.76

3.1.2 Dispersed phases

Two mineral oils of paraphinic base, the 500PS and the Drakeol 7, both provided by local company AGECOM were employed as dispersed phases. In the special case of Drakeol 7 (Transparent oil), a green aniline from Lacxe was used

to dye it (50 mg/L). The physicochemical properties of the oils were measured in the Laboratory for Fluids Characterization of PUC Rio and are summarized in Table 3.3.

Table 3. 3 Physicochemical properties of dispersed phases. T = 25 °C.

Property	Value	
	500PS	**Drakeol 7**
Density, Kg/m^3	882	845
Dynamic Viscosity, Pa.s	0.192	0.0178
Surface Tension, mN/m	30.3	28.3

3.1.3 Emulsion properties

The O/W emulsions evaluated in this investigation were formulated to two different dispersed phase concentration values, 0.5% and 5% (Volumetric basis). The more diluted emulsions were used predominantly in the visualization experiments, while 5% emulsions were used in the MSDD determination. In all cases, the surfactant based continuous phase was employed for preparation of the emulsions. Besides the dispersed phase concentration, emulsions were characterized by their drop size distribution, measured in a particle size analyzer. The DSD characterization method will be described in section 3.4.1.

3.2 Interfacial tension (IFT) experiments

As already discussed in section 2.2.2, the interfacial tension between continuous and dispersed phases plays a key role in the description of the drop breakup phenomenon. In this subsection, a brief explanation of the principles of the pendant drop technique and a description of the equipment used in the IFT measurements for studied systems is presented.

3.2.1 Pendant drop technique

The pendant drop technique is an experimental method used to determine surface or interfacial tensions based in the fact that small drops or bubbles tend to

be spherical, due to the predominance of surface forces over gravitational forces acting on them. However, if the drop is of a size such that surface tension and gravitational effects are comparable, the surface or interfacial tension can be determined from measurements of the shape of the drop or bubble (Adamson and Gast, 1997). A drop hanging from a tip (or a clinging bubble) elongates as it increases in size because the difference in hydrostatic pressure becomes significant in comparison with that given by the curvature of the drop. If the drop's expansion is stopped before gravity overcomes the surface tension (in which case the drop falls), and the drop is left undisturbed, a force balance will be attained and the final shape of the drop will depend on its size, the density difference between drop and its surroundings, and the surface/interfacial tension. With respect to Figure 3.1, this balance may be expressed by means of the Young-Laplace equation (Equation 3.1).

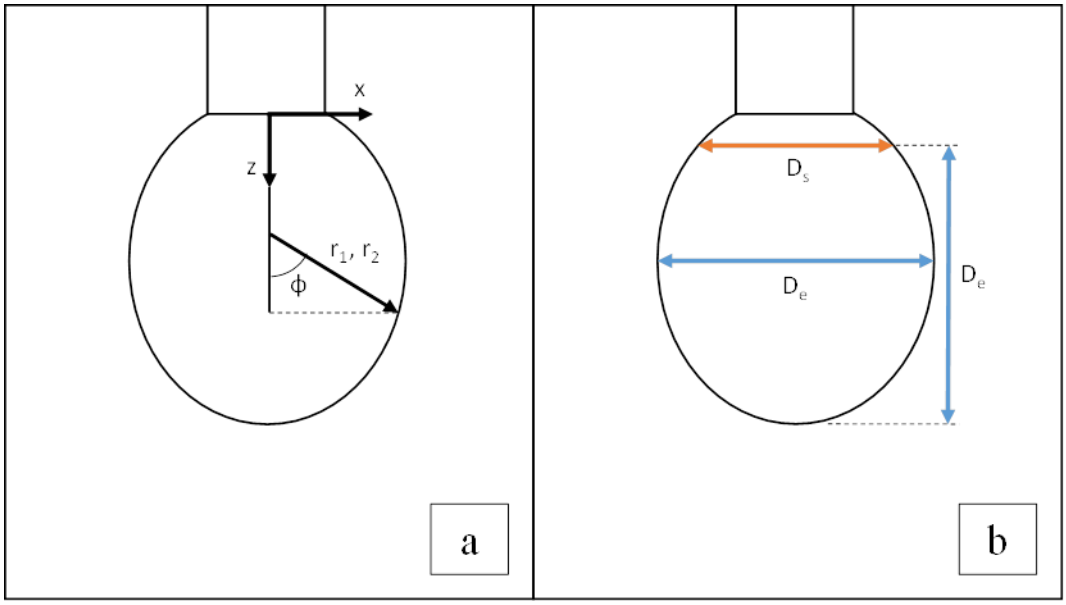

Figure 3. 1 (a) Coordinates system for the pendant drop geometry. (b) Drop measurements needed to calculate shape factor S.

$$\sigma\left(\frac{1}{r_1}+\frac{1}{r_2}\right)=\frac{2\sigma}{b}+\Delta\rho g z \tag{3.1}$$

Where r_1 is the radius of curvature on the x-z plane, r_2 is the radius of curvature on the plane normal to z, and b is the value of the radius of curvature at the apex of the drop (since the drop is symmetric, both curvature radii have the same value at the apex). If this equation is expressed as a function of the angle ϕ

of Figure 3.1(a), it is called the Bashforth-Adams equation (Hiemenz and Rajagopalan, 1997), which in dimensionless form is:

$$\frac{1}{\frac{r_1}{b}} + \frac{\sin\phi}{\frac{x}{b}} = 2 + B_0 \frac{z}{b} \tag{3.2}$$

Where B_0 is the Bond number (ratio of gravitational to surface forces acting on the drop) and is equal to:

$$B_0 = \frac{\Delta\rho g b^2}{\sigma} \tag{3.3}$$

Equation 3.2 can be solved numerically, with B_0 and ϕ as parameters. However, the exact value of b is hard to determine. Therefore, Adamson and Gast (1997) developed a simplified method based on the conveniently measurable shape dependent quantity S, which in accordance to Figure 3.1(b) is defined as:

$$S = \frac{D_s}{D_e} \tag{3.4}$$

Where D_e is the equatorial diameter of the drop and D_s is the diameter at a distance from the apex equal to D_e. The difficult to measure parameter b was combined with B_0 to define a new shape dependent variable, H:

$$H = B_0 \left(\frac{D_e}{b}\right)^2 \tag{3.5}$$

Which is a modified Bond number. This allows the surface tension to be calculated as:

$$\sigma = \frac{\Delta\rho g D_e^2}{H} \tag{3.6}$$

The relationship between H and S was determined experimentally, and a set of $1/H$ values versus S was obtained. Adamson and Gast (1997) found an extensive and reasonably accurate table of such values. Therefore, the only

information needed to calculate the surface or interface tension from the image of the drop is D_e, D_s, and $\Delta\rho$.

3.2.2
IFT measurements

To determine the interfacial tension between continuous and dispersed phases employed in the work of this dissertation, a Tracker tensiometer (TECLIS) based in the pendant drop technique was used (Figure 3.2).

Figure 3. 2 TRACKER (TECLIS) pendant drop tensiometer.

A halogen lamp was used as light source and placed behind the drop to increase the contrast between it and the background. The drops were formed inside a cuvette by means of a 250 µl SGE Analytical syringe equipped with a U-shaped needle. The cuvette was filled with the highest density liquid (aqueous phase), while the syringe contained the oil phase. The cuvette and the syringe were placed in thermostated cases attached to a Polyscience temperature controller (Heating Bath). The cuvette temperature was monitored by a K thermocouple inserted in a temperature probe located in the cuvette base.

The images of the drops were acquired by a Computar TEC-M55 55mm Telecentric Lens camera. This is a black and white, 2/3” CCD, analog camera, which was attached to a Cosmicar/Pentax 2X zoom lens that enhances and allows

the image to be properly focused. The camera converts the image into a RS-232 analog signal, which is transmitted to an Intel Core i3-2120 PC.

The tested liquids were those described in sections 3.1.1 and 3.1.2. Figure 3.3 shows results for systems with tap water as the continuous phase, while Figure 3.4 shows results for surfactant based systems. Table 3.4 summarizes the results of equilibrium IFT measurements for considered systems.

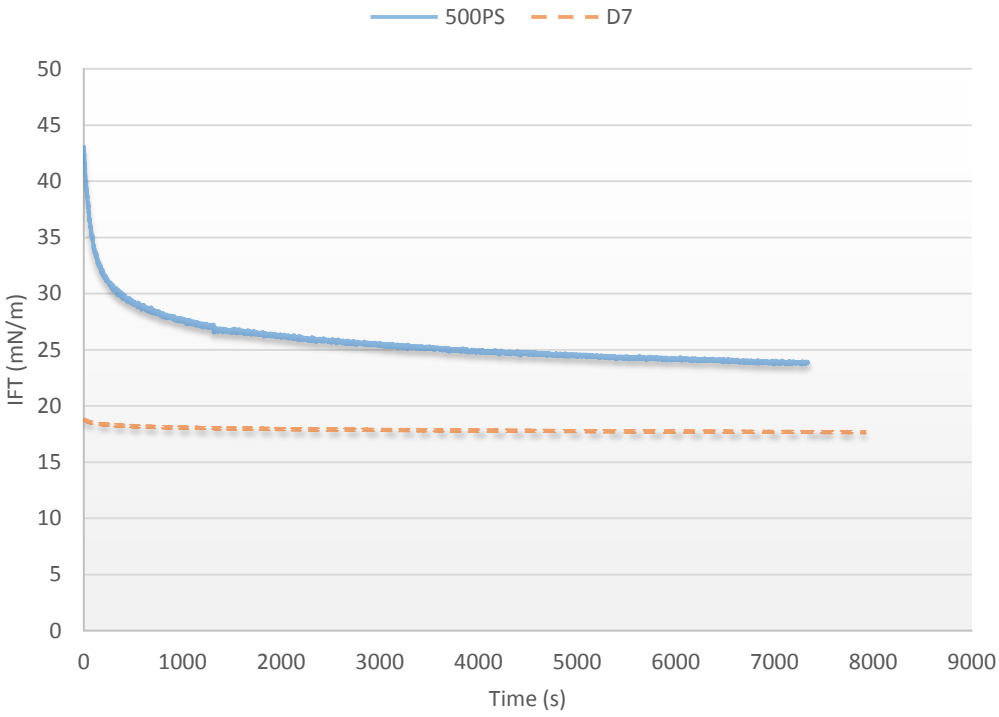

Figure 3. 3 Dynamic interfacial tension for dispersed phases in tap water as continuous phase. T = 25°C.

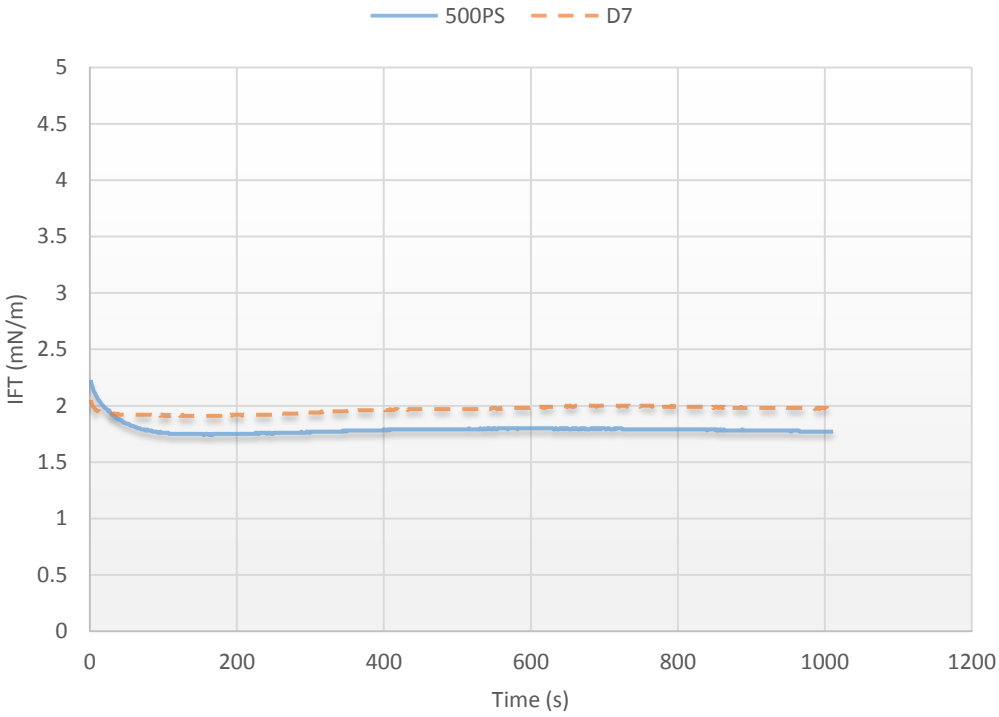

Figure 3. 4 Dynamic interfacial tension for dispersed phases in surfactant based continuous phase. T = 25°C.

Table 3. 4. Equilibrium interfacial tension for oil-water systems. T = 25°C.

O/W system	Interfacial tension (mN/m)
500PS/Tap water	24.51
Drakeol 7/Tap water	17.65
500PS/Surfactant based	1.79
Drakeol 7/Surfactant based	1.98

3.3
Experiments for visualization of drop breakup in turbulent flow

In this subsection, the equipment and experimental techniques considered for visualization of the breakup mechanisms in both cases evaluated in the work of this dissertation are described. In all cases, a Photron Fastcam SA3 high-speed camera and a LojaLab 150 W halogen backlight were used.

3.3.1
Visualization of drop breakup in a RSM

In this case, the high-speed camera was equipped with a Nikon PK – 12-auto extension ring and a Nikon AF Nikkor 50 mm f/1.4D lens. All video samples were recorded to 2000 frames per second (Δt = 0.5 ms, 768x1024 pixels and 512x512 pixels). The high-speed mixer was an IKA ULTRA TURRAX® T25 Basic RSM equipped with a S25N – 18G – ST dispersing element. Figure 3.5 shows a general view of the mixer (a), as well as its dispersing element (b) and a view from beneath where the rotor and rotor – stator gap can be observed (c). Tables 3.5 and 3.6 show the main characteristics of the mixer and the dispersing element, respectively.

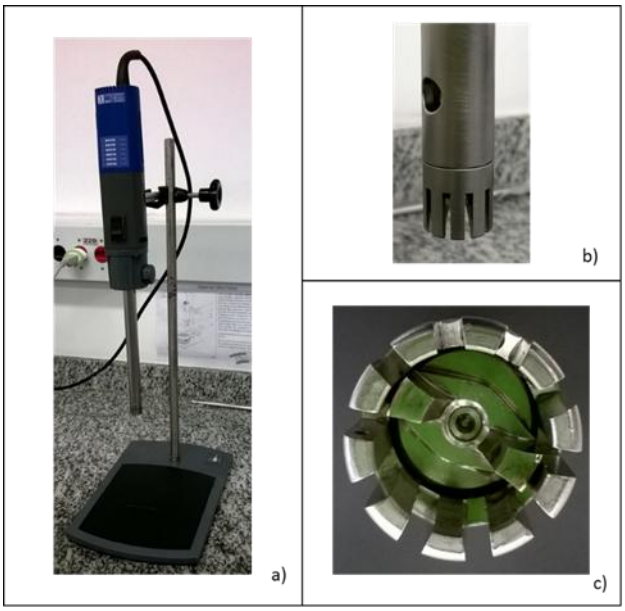

Figure 3. 5 (a) View of the IKA ULTRA TURRAX® T25 Basic mixer, (b) close up of the dispersing element, (c) view from beneath the dispersing element.

Table 3. 5 Technical data for IKA ULTRA TURRAX® T25 Basic mixer.

Technical data	
Speed range (rpm)	6500 – 24000
Speed display	Scale
Speed variation on load change (%)	< 6%
Perm. ambient temperature (°C)	5 – 40
Perm. humidity (%)	80
Power consumption (W)	500
Power output (W)	300
Design voltage (V)	230 ±10%
Frequency (Hz)	50/60
Dimensions (drive) WxDxH (mm)	65x80x240
Weight (Kg)	1.6

Table 3. 6 Technical data for S25N – 18G – ST dispersing element.

Technical data	
Volume range (L)	0.01 – 1.5
Stator diameter (mm)	18
Rotor diameter (mm)	13.4
Gap between rotor and stator (mm)	0.25
Allowable max. speed (rpm)	25000
Circumferential max. speed (m/s)	17.5
Shaft length (mm)	194
Material in contact with medium	PTFE, AISI 316L
pH range	2 – 13
Working max. temperature (°C)	180

Figure 3.6 shows the standard configuration used for experimental tests in the rotor – stator mixer.

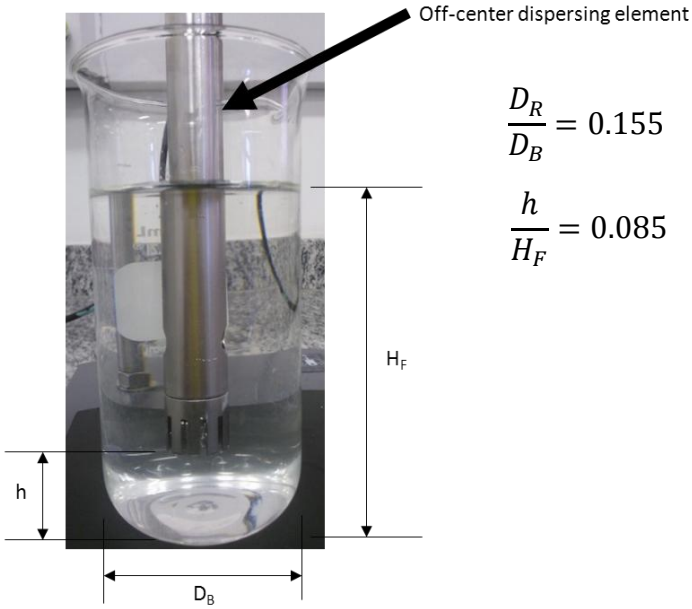

Figure 3. 6 Standard configuration for study the drop breakup process in a rotor – stator mixer.

The mixing vessel was a standard 600 mL beaker made of PYREX glass. The dispersing element was fixed off-center (to avoid the formation of a central vortex when the mixer is running) at a clearance equal to 8.5% of the fluid total height, from the bottom. The rotor diameter to beaker diameter ratio (D_R/D_B) was 0.155, based on the narrow section of the beaker. All experiments considered a total volume of 400 mL of an O/W emulsion with 0.5% in volume of oil. Emulsions were prepared adding dispersed phase to continuous phase.

Two different breakup cases were evaluated. First, the breakup of a 0.5% O/W dispersion was recorded for dyed Drakeol 7 and tap water as continuous phase for a mixing speed of 6500 rpm. Then, the breakup of a single droplet for different combinations of dispersed phase viscosity and interfacial tension was recorded for the same mixing speed. The oil droplets were generated controlling the flow rate in a Cole Parmer single Syringe-infusion Pump (115 VAC) and a Becton Dickinson 3 mL syringe equipped with a metallic hub needle as shown in Figure 3.7.

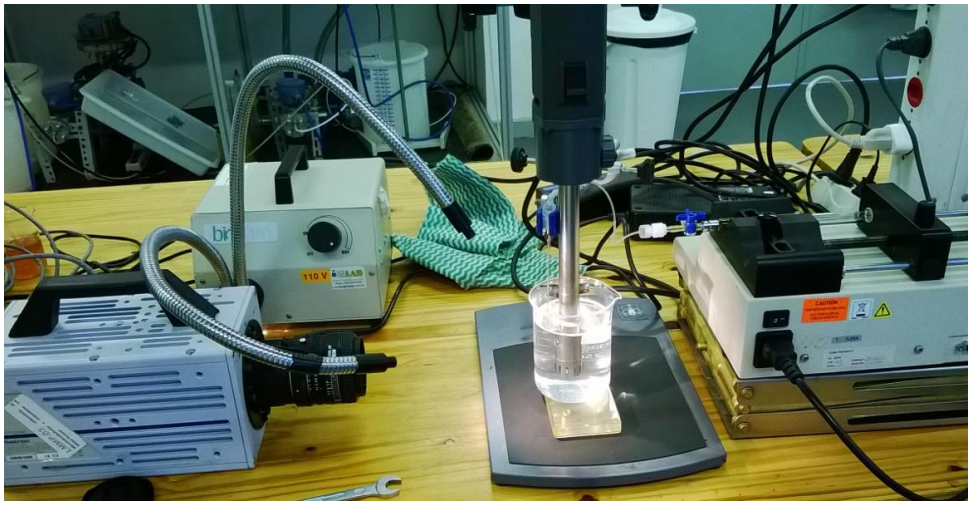

Figure 3. 7 Experimental set-up for the visualization of breakup mechanisms in a RSM. Single droplet case.

3.3.2
Visualization of drop breakup through an orifice

For visualization of single droplet breakup mechanisms through a restriction, the high-speed camera was equipped with an adapter tube (Navitar 2X F-mount) and a body tube zoom system (Navitar 6.5X Zoom, 12 mm FF). A schematic diagram of the liquid-liquid loop is shown in Figure 3.8. The experimental setup is a flow arrangement made of a standard ¼ in. 316L Swagelok tubing (ID = 4.57mm). The continuous phase was pumped from 60 L plastic tanks by a helical pump (Amboretto, Max. Flow Rate = 2 L/min, Max. Pressure = 2 bar, Motor Nominal Power = 2 CV) equipped with a WEG CFW08 frequency converter, and its flow rate was measured using a Micromotion R025S flow meter.

The dispersed phase (pure oil) was pumped by a Teledyne Isco 500D syringe pump connected to a metallic cylinder where oil was stored. As in the case of the mixer, the oil droplets were generated controlling the flow rate in the syringe pump. The dispersed phase was injected through a tee just before the restriction to avoid any external source of breakup (flow through tubing accessories). A set of transparent orifices (designed with different orifice diameter and length) was fabricated by local company Incomplast using high medium impact acrylic. Figure 3.9 shows the design of the orifices.

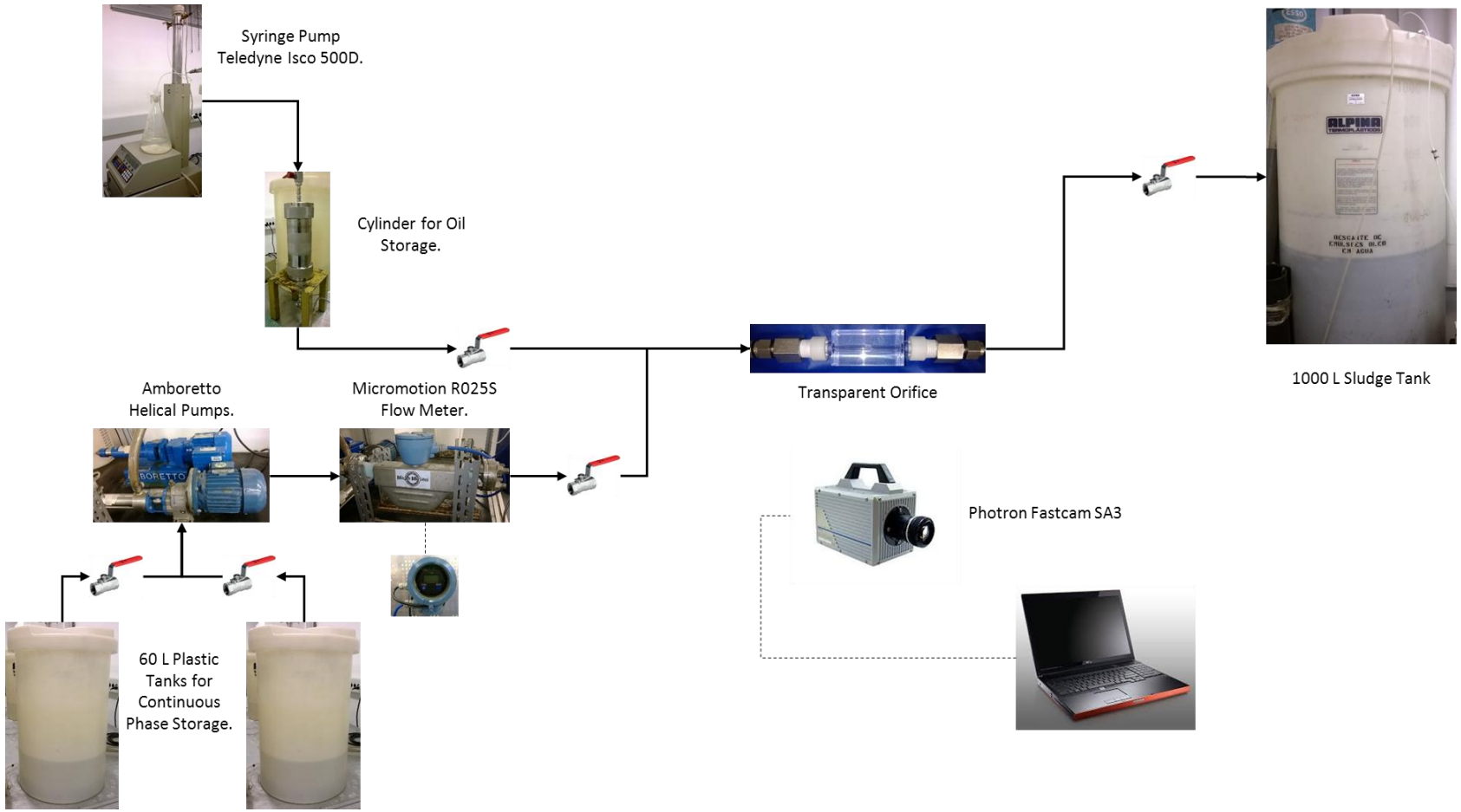

Figure 3. 8 Schematic diagram of experimental set-up for visualization of the breakup of a single oil droplet through an orifice**.**

To optimize the use of the light source, half of a two-inch PVC pipe was coated with a reflective cloth and placed behind of the transparent device (Figure 3.10). Videos were recorded to two different velocities, 1500 frames per second (1024x512 pixels) and 3000 frames per second (1024x256 pixels). Besides breakup mechanisms, the relative influence of dispersed phase viscosity, interfacial tension and geometry of the restriction in the breakup phenomenon was also studied.

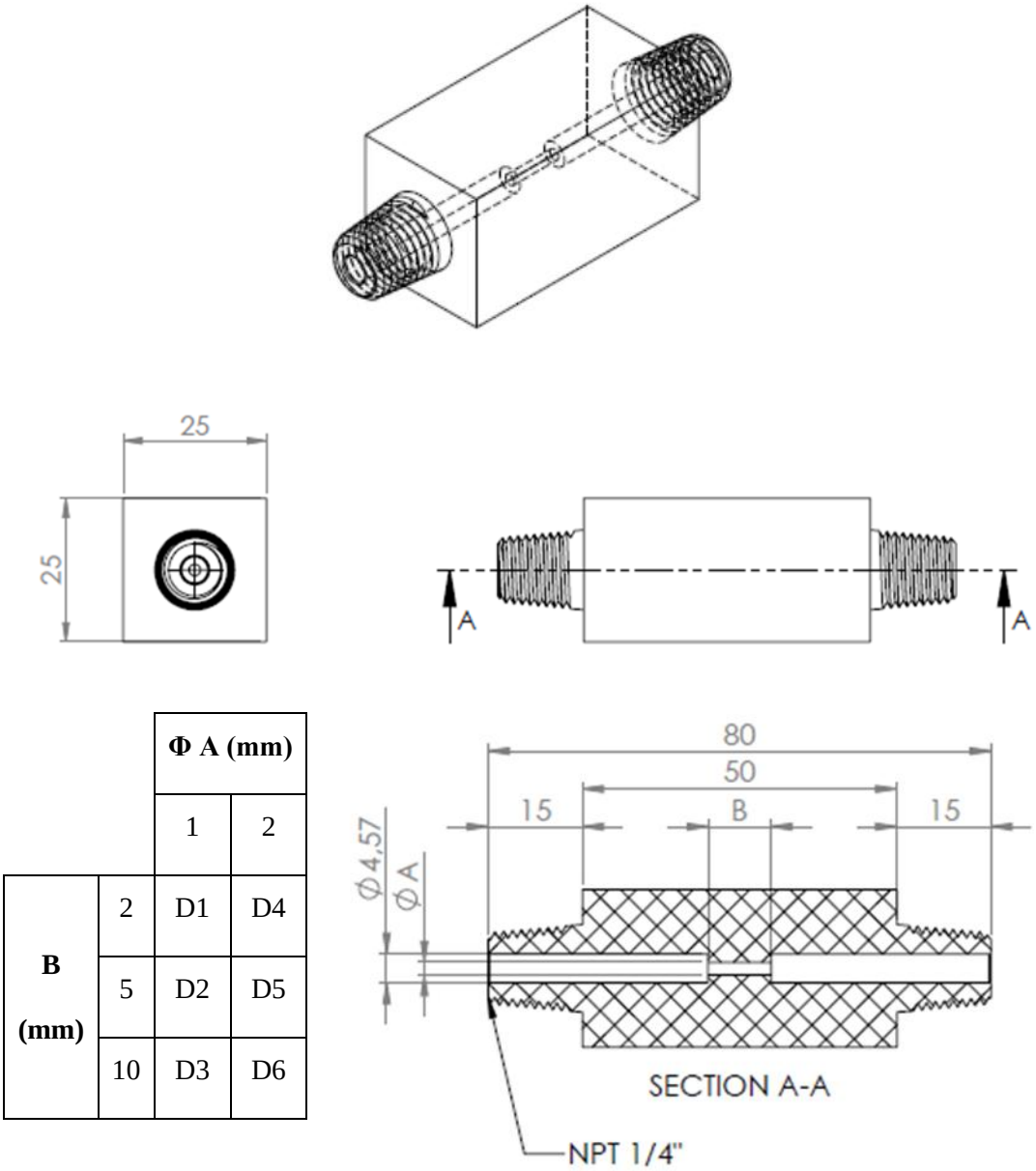

		Φ A (mm)	
		1	2
B (mm)	2	D1	D4
	5	D2	D5
	10	D3	D6

Figure 3. 9 Design of transparent device for visualization of turbulent drop breakup through an orifice.

Figure 3. 10 Experimental set-up for the visualization of breakup mechanisms in the flow through an orifice. Single droplet case.

3.4
Maximum Stable Drop Diameter (MSDD) experiments

In this subsection, the experimental techniques and equipment considered in determination of MSDD for the turbulent breakup of 5% O/W emulsions in both studied cases are described. As an introduction, the measurement principle of the Particle Size Analyzer is discussed.

3.4.1
Measurement of Drop Size Distribution (DSD)

DSD measurements were performed offline by laser diffraction technique using a Malvern Mastersizer 2000 Particle Size Analyzer coupled to a Malvern Hydro 2000MU dispersing unit. The device and the experimental procedures are presented herein.

3.4.1.1
Laser diffraction principle.

Laser diffraction measures DSD by measuring the angular variation in intensity of light scattered as a laser beam passes through a dispersed particulate sample. Large particles scatter light at small angles relative to the laser beam and

small particles scatter light at large angles. The angular scattering intensity data is then analyzed to calculate the size of the particles responsible for creating the scattering pattern, using the Mie theory, assuming a spherical volume equivalent model. Mie theory requires knowledge of the optical properties (refractive index and imaginary component) of both the sample being measured, along with the refractive index of the dispersant. Usually the optical properties of the dispersant are relatively easy to find from published data, and many modern instruments will have in-built databases that include common dispersants. For samples where the optical properties are not known, the user can either measure them or estimate them using an iterative approach based upon the goodness of fit between the modeled data and the actual data collected for the sample. Figure 3.11 shows the fundamentals of laser diffraction technique for particle size measurement.

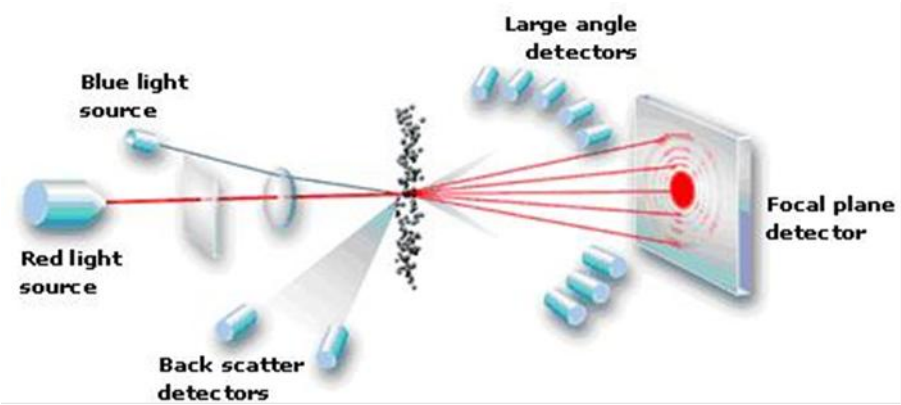

Figure 3. 11 Laser diffraction technique to determine DSD. Taken from http://particle.dk/methods-analytical-laboratory/particle-size-by-laser-diffraction/laser-diffraction-theory/

3.4.1.2 Particle size analyzer

As already stated, the determination of DSD was performed by a Malvern Mastersizer 2000 Particle Size Analyzer coupled with a Malvern Hydro 2000MU dispersing unit (Figure 3.12).

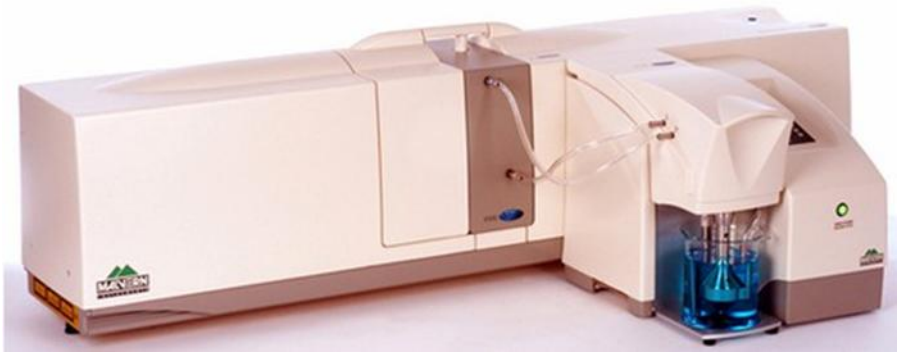

Figure 3. 12 Malvern Mastersizer 2000 particle analyzer and Malvern Hydro 2000MU dispersing unit.

The Mastersizer 2000 is designed to work with materials in the size range of 0.02 – 2000 µm. It is equipped with forward, side and back scattering detection systems for red light and wide angle forward and back scattering detection systems for blue light. It also uses a helium-neon laser as source of red light; a solid-state light source for blue light and an automatic rapid optical align system with dark field optical reticle.

The Hydro 2000MU is a semi-automated large volume-dispersing unit designed for the measurement of dense, large materials or polydisperse distributions. It has a dip-in pump and a stirrer head that allows measurements to be carried out in a standard laboratory beaker (600 and 1000 mL).

3.4.1.3 DSD measurement

To perform a DSD measurement, the sample was initially introduced in the dispersion unit. The dispersion unit then pumps the dispersed sample to the measurement cell (Figure 3.13) where the scattered laser light is measured. The stirrer speed of the dispersion unit was adjusted to 2000 rpm, and the sample was added using a 3 mL plastic pipette until the laser obscuration reached a value between 12 and 15%. To the Mastersizer calculate the sample DSD from the light scattering data, it required to know the refractive indices of the continuous and dispersed phases. The refractive indices were selected from the database of refractive indices of materials embedded in the software provided by the manufacturer. Normally, the Mastersizer perform three measurements per sample,

and calculate an averaged DSD, which is used as the final DSD of the evaluated sample.

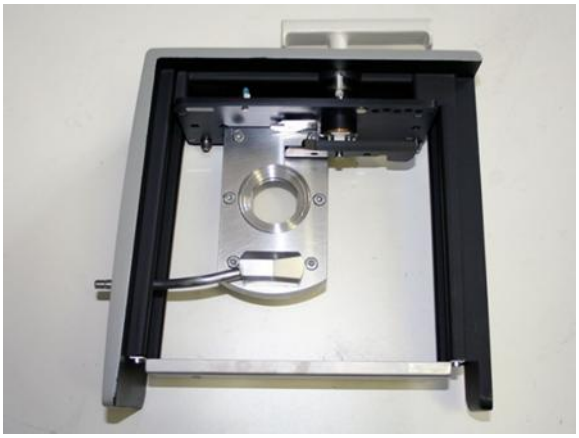

Figure 3. 13 Measurement cell of the Malvern Mastersizer 2000.

3.4.2
MSDD experiments for drop breakup in a rotor – stator mixer

Maximum stable drop size data were determined for the breakup of O/W emulsions with a concentration of 5% of dispersed phase in a Rotor – Stator Mixer using the standard configuration shown in Figure 3.6. The drop size distribution of emulsions obtained to four different mixing speeds (6500, 9500, 13500 and 17500 rpm) and various mixing times were measured. In this case, it was assumed that the MSDD was achieved at sufficiently high mixing time.

3.4.3
MSDD experiments for drop breakup through an orifice

The experimental setup used to investigate the drop breakup through an orifice is described in this subsection. In the setup, an O/W emulsion with a concentration of 5% of dispersed phase (formed inline) flowed through a transparent device, which contain the orifice (Orifice Diameter = 1 mm, Orifice Length = 5 mm). The DSD upstream and downstream of the restriction was measured in a particle size analyzer for various flow conditions.

A schematic diagram of the liquid – liquid loop is shown in Figure 3.14. The dispersed phase was pumped in the form of a concentrated emulsion by the Teledyne Isco 500D syringe pump. To assure the dispersed phase stability under storage conditions (prevent creaming process), a concentrated emulsion (87% in

volumetric basis) was prepared from an original 50% emulsion, whose d_{90} was corresponding to the required d_{90} upstream of the orifice (adjusted in the RSM as a function of mixing speed and time conditions). Then, this 50% emulsion was aged for one day in a separation funnel of PYREX glass (where it is concentrated up to 87%). The concentrated emulsion was removed from the funnel and poured into the metallic cylinder for storage. After that, its DSD was measured just to discard structural changes. Finally, the concentrated emulsion and continuous phase flow rates were adjusted to get an emulsion stream with an oil concentration of 5%, before entering the orifice.

The pressure drop through the restriction was measured by a Dwyer 490 Wet-Wet differential manometer (pressure range of 0 – 100 psi) and sample takers located upstream and downstream of the orifice were used to determine the difference of DSD for different flow rate values. The discarded emulsion volume was redirected to a 1000 L sludge tank.

The MSDD for each set of flow conditions was found evaluating the difference between the DSD obtained upstream and downstream the restriction. In a mathematical form, MSDD was the d_{90} value of the DSD when it matches the following criterion:

$$\Delta(d_{10}, d_{50}, d_{90}\ and\ d_{32}) < 1\ \mu m \tag{3.7}$$

Equation 3.7 means that MSDD for a given sample is the d_{90} value of the downstream distribution when the difference between the upstream and downstream DSD (calculated as the change of the d_{10}, d_{50}, d_{90} and d_{32} values), is lower than one micrometer (1 μm).

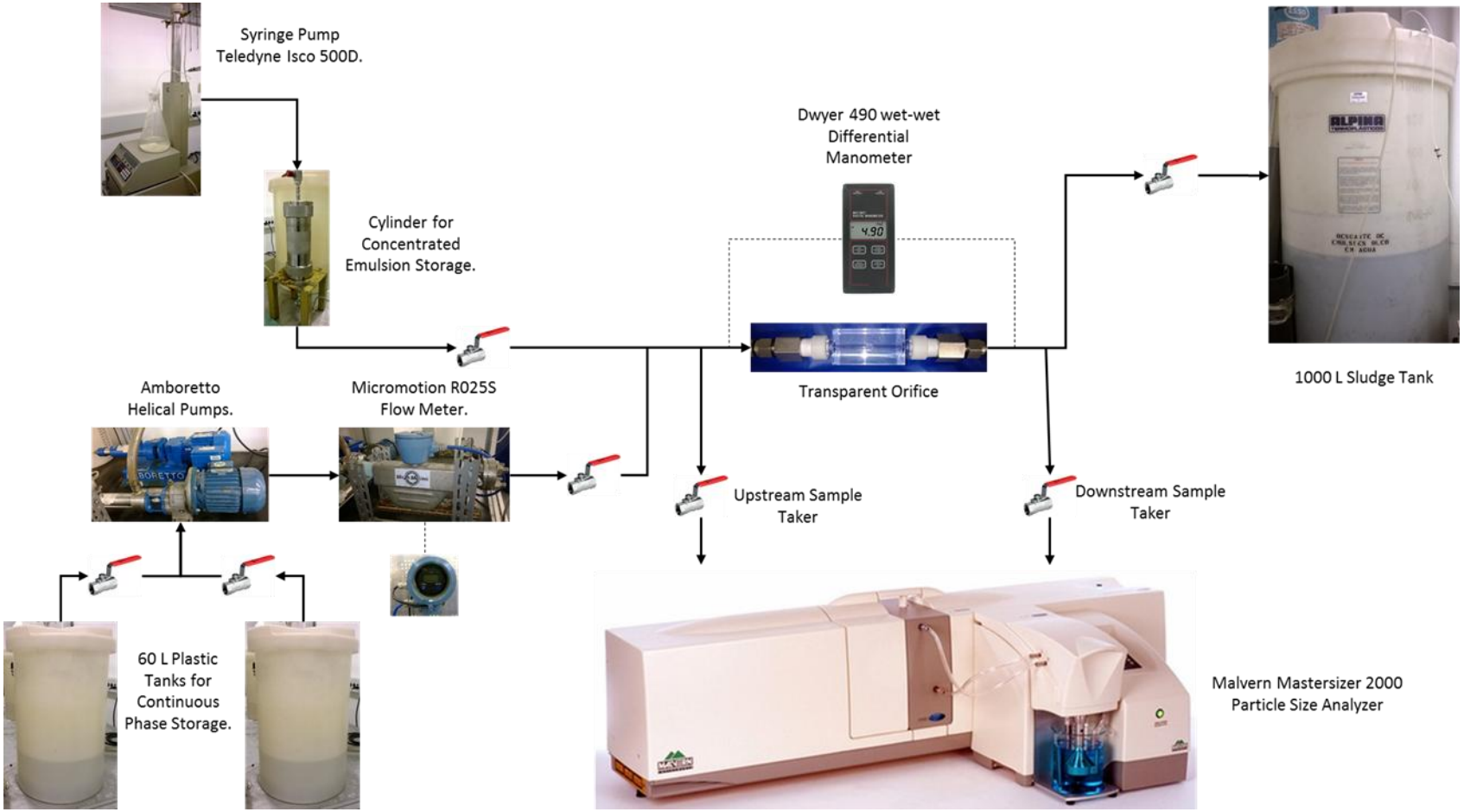

Figure 3. 14 Schematic diagram of experimental set-up for determination of MSDD for drop breakup of diluted O/W emulsions through an orifice.